SOUTHERN PLAINS
TRANSPORTATION CENTER

Infrastructure-Relevant Climate Projections for the Southern Great Plains

Katharine Hayhoe, Ph.D.
Darryl James, Ph.D.
Anne Stoner, Ph.D.
Bhagya Athukorallage, Ph.D.

SPTC15.5-04-F

Southern Plains Transportation Center
201 Stephenson Parkway, Suite 4200
The University of Oklahoma
Norman, Oklahoma 73019

DISCLAIMER

The contents of this report reflect the views of the authors, who are responsible for the facts and accuracy of the information presented herein. This document is disseminated under the sponsorship of the Department of Transportation University Transportation Centers Program, in the interest of information exchange. The U.S. Government assumes no liability for the contents or use thereof.

TECHNICAL REPORT DOCUMENTATION PAGE

1. REPORT NO.	2. GOVERNMENT ACCESSION NO.	3. RECIPIENTS CATALOG NO.
SPTC15.5-04		

4. TITLE AND SUBTITLE	5. REPORT DATE
Infrastructure-Relevant Climate Projections for the Southern Great Plains	February 23, 2018
	6. PERFORMING ORGANIZATION CODE
7. AUTHOR(S)	8. PERFORMING ORGANIZATION REPORT
Katharine Hayhoe, Ph.D., Darryl James, Ph.D., Anne M.K. Stoner, Ph.D., Bhagya Athukorallage, Ph.D.	
9. PERFORMING ORGANIZATION NAME AND ADDRESS	10. WORK UNIT NO.
Texas Tech University 2500 Broadway, Lubbock, Texas 79409	11. CONTRACT OR GRANT NO. DTRT13-G-UTC36
12. SPONSORING AGENCY NAME AND ADDRESS	13. TYPE OF REPORT AND PERIOD COVERED
Southern Plains Transportation Center 201 Stephenson Pkwy, Suite 4200 The University of Oklahoma Norman, OK 73019	Final June 2017 – December 2018
	14. SPONSORING AGENCY CODE

15. SUPPLEMENTARY NOTES

University Transportation Center

16. ABSTRACT

Transportation infrastructure is typically designed and built based on the assumption that the risks associated with climate and weather conditions at any given location do not change over time. Today, however, climate change is altering the risk of many types of weather extremes including the frequency and/or severity of high temperatures, heavy precipitation events, coastal flooding, and storms. Here, we developed maps of typical climate indices expected to impact a large variety of infrastructure structures and performed a quantitative analysis assessing how climate change may impact pavement performance and thermal conductivity in the Southern Plains as well as in other locations within the continental U.S. by applying state-of-the-art climate projections to generate infrastructure-relevant data products that will allow transportation researchers to assess and prepare for the potential risks a changing climate poses to Southern Plains roads, highways, bridges, culverts, and other infrastructure. The unique results indicate that increasing temperatures have a negative effect on flexible pavements for the majority of the locations included here for all measures of deformation as well as increases to the temperature gradient within the asphalt structure, which is more pronounced under warmer temperatures. Studies such as these, along with the regional and national maps of specific indicators, should help guide infrastructure planners and designers when building new roads and other infrastructure to ensure it is built to withstand current and future warming trends.

17. KEY WORDS	18. DISTRIBUTION STATEMENT
Climate change, climate indices, flexible pavement, infrastructure, pavement performance	No restrictions. This publication is available at www.sptc.org and from the NTIS.

19. SECURITY CLASSIF. (OF THIS REPORT)	20. SECURITY CLASSIF. (OF THIS PAGE)	21. NO. OF PAGES	22. PRICE
Unclassified	Unclassified	45	

SI* (MODERN METRIC) CONVERSION FACTORS

APPROXIMATE CONVERSIONS TO SI UNITS

SYMBOL	WHEN YOU KNOW	MULTIPLY BY	TO FIND	SYMBOL
		LENGTH		
in	inches	25.4	millimeters	mm
ft	feet	0.305	meters	m
mi	miles	0.914	meters	m
yd	yards	1.61	kilometers	km
		AREA		
in^2	square inches	645.2	square millimeters	mm^2
ft^2	square feet	0.093	square meters	m^2
yd^2	square yards	0.836	square meters	m^2
ac	acres	0.405	hectares	ha
mi^2	square miles	2.59	square kilometers	km^2
		VOLUME		
fl oz	fluid ounces	29.57	milliliters	mL
gal	gallons	3.785	liters	L
ft^3	cubic feet	0.028	cubic meters	m^3
yd^3	cubic yards	0.765	cubic meters	m^3
		NOTE: Volumes greater than 1000L shall be shown in m^3		
		MASS		
oz	ounces	28.35	grams	g
lb	pounds	0.454	kilograms	kg
T	short tons (2000 lb)	0.907	megagrams (or “metric ton”)	Mg (or “t”)
		TEMPERATURE (exact degrees)		
°F	Fahrenheit	5(F-32)/9 or (F-32)/1.8	Celsius	°C
		ILLUMINATION		
fc	foot-candles	10.76	lux	lx
fl	foot-Lamberts	3.426	candela/m^2	cd/m^2
		FORCE and PRESSURE or STRESS		
lbf	poundforce	4.45	newtons	N
lbf/in^2	poundforce per square inch	6.89	kilopascals	kPa

APPROXIMATE CONVERSIONS FROM SI UNITS

SYMBOL	WHEN YOU KNOW	MULTIPLY BY	TO FIND	SYMBOL
		LENGTH		
mm	millimeters	0.039	inches	in
m	meters	3.28	feet	ft
m	meters	1.09	yards	yd
km	kilometers	0.621	miles	mi
		AREA		
mm^2	square millimeters	0.0016	square inches	in^2
m^2	square meters	10.764	square feet	ft^2
m^2	square meters	1.195	square yards	yd^2
ha	hectares	2.47	acres	ac
km^2	square kilometers	0.386	square miles	mi^2
		VOLUME		
mL	milliliters	0.034	fluid ounces	fl oz
L	liters	0.264	gallons	gal
m^3	cubic meters	35.314	cubic feet	ft^3
m^3	cubic meters	1.307	cubic yards	yd^3
		MASS		
g	grams	0.035	ounces	oz
kg	kilograms	2.202	pounds	lb
Mg (or “t”)	megagrams (or “metric ton”)	1.103	short tons (2000 lb)	T
		TEMPERATURE (exact degrees)		
°C	Celsius	1.8C + 32	Fahrenheit	°F
		ILLUMINATION		
lx	lux	0.0929	foot-candles	fc
cd/m^2	candela/m^2	0.2919	foot-Lamberts	fl
		FORCE and PRESSURE or STRESS		
N	newtons	0.225	poundforce	lbf
kPa	kilopascals	0.145	poundforce per square inch	lbf/in^2

Infrastructure-Relevant Climate Projections for the Southern Great Plains

Final Report

February 2019

Principal Investigator: Katharine Hayhoe, Ph.D.

Co-Principal Investigators: Darryl James, Ph.D. and Anne Stoner, Ph.D.

Coauthor: Bhagya Athukorallage, Ph.D.

Texas Tech University

Lubbock, TX 79409

Southern Plains Transportation Center

University of Oklahoma

201 Stephenson Pkwy, Suite 4200

Norman, OK 73019

SPTC15.5-04

TABLE OF CONTENTS

LIST OF FIGURES

LIST OF TABLES

EXECUTIVE SUMMARY

Transportation infrastructure is typically designed and built based on the assumption that the risks associated with climate and weather conditions at any given location do not change over time. Today, however, climate change is altering the risk of many types of weather extremes including the frequency and/or severity of high temperatures, heavy precipitation events, coastal flooding, and storms. A crucial element of infrastructure planning is the environmental conditions that will occur over the lifetime of each component, including both mean climate and average variability. Each structure is designed with enough flexibility and capacity to withstand fluctuations around a mean state, including most historically observed extreme events, such as prolonged heat waves or sudden downpours. However, if over the lifetime of the structure the mean state of its environment and/or the range of variability it experiences are not stationary or stable, to maintain longevity and user safety infrastructure design guidelines will need to account for that non-stationarity as well as any projected future change. Failure to do so will compromise the integrity and the lifetime of the structure.

Here, we developed maps of typical climate indices expected to impact a large variety of infrastructure structures and performed a quantitative analysis assessing how climate change may impact pavement performance and thermal conductivity in the Southern Plains as well as in other locations within the continental U.S. by applying state-of-the-art climate projections to generate infrastructure-relevant data products that will allow transportation researchers to assess and prepare for the potential risks a changing climate poses to Southern Plains roads, highways, bridges, culverts, and other infrastructure.

Outcomes specific to the objectives in the proposal are: (1) the development of a comprehensive understanding of the sensitivity of Southern Plains infrastructure to weather and climate through a comprehensive literature review; (2) the generation of a probabilistic ensemble of high-resolution climate projections for the region, using state-of-the-art methods that account for uncertainty in natural variability, scientific understanding, and the human emissions driving future change; (3) the translation of these projections into indicators of aspects of climate that affect Southern Plains infrastructure; and (4) the provision of this information to modeling of flexible pavement performance and heat transfer; and (5) the

revision and development of the final climate products, which will be made available to regional users via an easily accessible interface that can be integrated with geographic information systems analysis hosted by the Environmental Systems Research Institute (ESRI).

The unique results indicate that increasing temperatures have a negative effect on flexible pavements for the majority of the locations included here for all measures of deformation as well as increases to the temperature gradient within the asphalt structure, which is more pronounced under warmer temperatures, echoing the findings of Mills et al. (*3*) and Meagher et al. (*4*). Locations in the Southern Plains show significant increases in permanent deformation, where warming temperatures cause the asphalt material to soften, increasing the potential for rutting, which in return results in lower expected lifetime of the pavement, with the time when metrics of failure is reached happening between four to six years earlier than observed presently. Increases in end-of-century AC and total permanent deformation tend to be positively correlated with temperature increases; i.e. locations that are projected to experience more warming also have the largest increase in permanent deformation relative to the baseline period.

Although these results present a broad overview of how climate could impact flexible pavement performance, more research is needed to understand how the changes in different climate variables, cause the pavement performance to change. Studies are also needed to examine how individual changes in the pavement structure and materials may enhance the pavement performance. This could lead to understanding how individual locations might alter the design, materials, and performance grade binder to optimize the performance and lifetime of the pavement.

In addition, these results demonstrate how GCM output can be translated into the information required to simulate pavement performance and demonstrate that there is a risk if future climate conditions are ignored, and highlighting the critical importance of more research in this area. Studies such as these, along with the regional and national maps of specific indicators, should help guide infrastructure planners and designers when building new roads and other infrastructure to ensure it is built to withstand current and future warming trends.

INTRODUCTION

Transportation infrastructure is typically designed and built on the assumption that the risks associated with climate and weather conditions at any given location do not change over time. This assumption underpins most design standards, operations and maintenance programs, and planning for transportation projects and programs. Today, however, climate change is altering the risk of many types of weather extremes including the frequency and/or severity of high temperatures, heavy precipitation events, coastal flooding, and storms. This concept of *non-stationarity*, that future climate conditions and weather risks will differ from those experienced in the past, challenges scientists and engineers to incorporate a changing climatic baseline into present-day planning.

A crucial element of infrastructure planning is the environmental conditions that will occur over the lifetime of each component, including both mean climate and average variability. Each structure is designed with enough flexibility and capacity to withstand fluctuations around a mean state, including most historically observed extreme events, such as prolonged heat waves or sudden downpours. However, if over the lifetime of the structure the mean state of its environment and/or the range of variability it experiences are not stationary or stable, to maintain longevity and user safety infrastructure design guidelines will need to account for that non-stationarity as well as any projected future change. Failure to do so will compromise the integrity and the lifetime of the structure.

As stated in the Transportation Research Board Special Report 290, *Potential Impacts of Climate Change on U.S. Transportation* (NRC, 2008): "The past several decades of historical regional climate patterns commonly used by transportation planners to guide their operations and investments may no longer be a reliable guide for future plans. In particular, future climate will include new classes (in terms of magnitude and frequency) of weather and climate extremes, such as record rainfall and record heat waves, not experienced in modern times as human-induced changes are superimposed on the climate's natural variability." Despite decades' worth

of research into climate modeling, uncertainty quantification, and generation of high-resolution future projections at temporal and spatial scales relevant to infrastructure design, however, very little of that growing knowledge has been incorporated into planning and design. A 2007 report from the National Research Council states: “Discovery science and understanding of the climate system are proceeding well but use of that knowledge to support decision making and to manage risks and opportunities of climate change is proceeding slowly.” (NRC, 2007)

How can this vast body of climate information be effectively incorporated into an even vaster body of information on infrastructure design and maintenance? NRC (2008) recommends three concrete steps. The first step is for infrastructure managers and owners -- including federal, state, and local – to inventory critical transportation infrastructure, including ports, airports, and rail facilities, to determine whether, when, and where projected climate changes in their regions might be consequential. The second step is for providers to incorporate climate change into their long-term capital improvement plans, facility designs, maintenance practices, operations, and emergency response plans. The third step is for planners and engineers to expand application and use of probabilistic investment analyses and design approaches that incorporate techniques for trading off the costs of making the infrastructure more robust against the economic costs of failure.

Despite pre-existing experiences of planning for an unpredictable future, the main obstacle associated with changing building codes and guidelines is uncertainty: in the management, the engineering, and the climate science. How will the usage, such as traffic or load, of the component change? How will the material react under different climatic conditions? And how will climate change in the future? Despite these uncertainties, it is clear from observed and projected future climate trends that assumptions of stationarity – that past climate serves as a reliable guide to the future – are becoming increasingly untenable, to the point where even when the full range of uncertainty associated with future projections is incorporated into future planning, it does not encompass recent historical conditions. These questions motivated and guided our proposed objective to develop and incorporate quantitative and probabilistic climate projections into evaluation and assessment of Southern Plains transportation

infrastructure and research.

Here, we performed a quantitative analysis assessing how climate change may impact Southern Plains infrastructure as well as infrastructure in other locations in the continental U.S. by applying state-of-the-art climate projections to generate infrastructure-relevant data products that will allow transportation researchers to assess and prepare for the potential risks a changing climate poses to Southern Plains roads, highways, bridges, culverts, and other infrastructure. The objective of this project was to assess the potential future impacts of climate non- stationarity on the Southern Plains region and explore the extent to which it is possible to develop relevant data products that enable climate projections to be incorporated into the design, building, and maintenance of a transportation infrastructure that will be resilient in the face of a changing climate. Outcomes specific to the objectives in the proposal are: (1) the development of a comprehensive understanding of the sensitivity of Southern Plains infrastructure to weather and climate through a comprehensive literature review; (2) the generation of a probabilistic ensemble of high-resolution climate projections for the region, using state-of-the-art methods that account for uncertainty in natural variability, scientific understanding, and the human emissions driving future change; (3) the translation of these projections into indicators of aspects of climate that affect Southern Plains infrastructure; and (4) the provision of this information to modeling of flexible pavement performance and heat transfer; and (5) the revision and development of the final climate products, which will be made available to regional users via an easily accessible interface that can be integrated with geographic information systems analysis hosted by the Environmental Systems Research Institute (ESRI).

PROPOSAL TASKS

TASK ONE. Literature Review and Online Survey

A literature review was conducted, examining the use of climate information and projections in infrastructure engineering research in the U.S. The review is currently going through final internal review and will be submitted for publishing to the Transportation Research journal in

January of 2019. The review concludes that although some progress has been made to assess the impact of future climate change on infrastructure assets, such as pavement, bridges, and culverts, not much has been done in terms of updating current standards and designs or retrofitting in-situ assets to accommodate for imminent changes in the climate. The original proposal had included an online survey but as the timing of the proposal funding was delayed, this survey was replaced with a more detailed literature review that was expanded to include all available information across the U.S., not only in the Southern Plains region.

TASK TWO. Develop High-Resolution Regional Climate Projections

Understanding the process by which high-resolution climate projections are generated and the main sources of uncertainty inherent to this process, including natural variability, scientific or model uncertainty, and scenario or human uncertainty, is an important step towards accounting for uncertainty in future projections and incorporating that information into future planning in a robust and relevant way. Development of future high-resolution climate indicators in a manner consistent with assessing the uncertainty in projected change requires: (1) future scenarios that describe how human activities may affect global climate; (2) global climate model simulations to translate future scenarios into regional climate; (3) a statistical downscaling model that is able to resolve the relationship between large-scale regional change and local impacts at an appropriate spatial and temporal scale for the desired outputs, and (4) long-term historical observations that can be used to train the statistical model.

Future scenarios depend on a myriad of factors, including how human societies and economies will develop over the coming decades; what technological advances are expected; which energy sources will be used in the future to generate electricity, power transportation, and serve industry; and how all these choices will affect future emissions from human activities. Because it is not possible to predict the future, we propose to develop future projections based on both a higher and lower scenario. The lower scenario demonstrates the necessity of adaptation; the higher scenario, the benefits of mitigation. The 2017/2018 Fourth U.S. National Climate Assessment compares climate changes under the Representative Concentration Pathways (RCP) higher 8.5 and lower 4.5 scenarios. Here, we propose to develop projections for the Southern

Great Plains using both of these RCP 8.5/4.5 scenarios to ensure that we cover a range of plausible futures, and that this range is compatible with existing and upcoming assessments at the regional to national scale.

Future scenarios are used as input to global climate models (GCMs). As output, GCMs produce geographic grid-based projections of temperature, precipitation, and other climate variables at daily and monthly scales. The newest generation of global models, CMIP5, served as input to the IPCC 5th assessment report (IPCC, 2013) as well as the Third and Fourth U.S. National Climate Assessments (Melillo et al., 2014; USGCRP, 2017). In this study, we developed climate projections based on global models that meet the following criteria. First, only well-established models were considered, those already extensively described and evaluated in the peer-reviewed scientific literature. Models must have been evaluated and shown to adequately reproduce key features of the atmosphere and ocean system. Second, the models should encompass the greater part of the IPCC range of uncertainty in climate sensitivity (2 to 4.5^{o}C; IPCC, 2007). Climate sensitivity is defined as the temperature change resulting from a doubling of atmospheric carbon dioxide concentrations relative to pre-industrial times, after the atmosphere has had decades to adjust to the change. The third and last criterion is that the models chosen must have continuous daily time series of temperature and precipitation archived for the scenarios used here (for CMIP5, RCP 8.5 and 4.5). The thirteen GCMs recommended for this analysis are the only models in the CMIP5 archives that meet these three criteria, having a proven track record of adequate performance in previous modeling inter-comparison projects: CanCM4, CCSM4, CNRM-CM5, CSIRO-Mk3.6.0, GFDL CM3, GISS E-H, GISS E-R, HadGEM2-ES, INMCM4, IPSL-CM5, Miroc5, MPI-ESM, MRI-CGCM3.

To translate GCM output into high-resolution, regionally relevant information, we applied the recently updated version 2 of the Asynchronous Regional Regression Model (ARRM) for daily temperature values. The previous ARRM v1 was used to downscale daily values of precipitation. ARRM v1 (Stoner et al., 2013) was used in previous U.S. National Climate Assessments and the Department of Transportation's Gulf Coast Study and uses piecewise linear asynchronous regression to create monthly models translating low-resolution GCM output to high-resolution

projections. ARRM v2 (Scott-Fleming et al., in preparation) combines the benefits of the previous model with new computational advances that improve model performance and better account for extremes. It offers flexible and computationally efficient approach to downscale station-based or gridded daily values of any variable that can be transformed into an approximately symmetric distribution and for which a large-scale predictor exists. By replacing the core statistical method, a parametric quantile regression, with a non-parametric kernel density estimation approach, ARRMv2 significantly improves the stationarity of the downscaling model as well as improving its computational efficiency by more than an order of magnitude, to the point where global simulations can be downscaled using a desktop computer in a matter of hours rather than weeks. Using the perfect model evaluation framework (Dixon et al., 2016), we have demonstrated how this method offers significant improvement and robustness over other commonly used statistical techniques including both empirical and parametric quantile regression (Hayhoe et al., in preparation). Overall, the new KDE-based technique is highly efficient, extremely robust even under a relatively large change in climate for temperature, and highly generalizable across geographic regions.

Finally, training the statistical downscaling model requires long time series of observations across the Southern Great Plains. Here, we generated projections corresponding to two different datasets. The first is a dataset of daily projections corresponding to a continuous 1/16th degree grid covering the entire Southern Great Plains region, encompassing the states of Texas, Oklahoma, Louisiana and New Mexico. These projections are based on 61 years (1950-2010) of assimilated meteorological data from: http://www.hydro.washington.edu/Lettenmaier/Data/livneh/livneh.et.al.2013.page.html. The second dataset consists of daily point-source projections corresponding to all individual weather stations from the Global Historical Climatology Network, which was additionally filtered using our quality control algorithm to identify and remove erroneous values that we have previously noted in the GHCN database. High-resolution gridded and individual station projections were generated for 25 GCMs for both temperature and precipitation for a lower and a higher future representative pathway (RCP4.5 and 8.5).

The final result of this work is a collection of daily and hourly climate variables generated for the GFDL-ESM2G climate model and the higher RCP8.5 scenario between 1950-2100 for 25 weather stations, listed in Table 1, across the continental U.S. The climate variables are listed below:

Daily statistically downscaled and bias-corrected values of

- Maximum temperature
- Minimum temperature
- Total precipitation amounts
- Maximum relative humidity
- Minimum relative humidity

Hourly disaggregated values of

- Temperature
- Precipitation amounts
- Relative humidity
- Wind speed
- Percent sunshine

Table 1. Weather stations used in pavement performance calculations.

City	WBAN Identifier	Latitude	Longitude
Phoenix, AZ	23183	33.4430	-111.9900
San Francisco, CA	23234	37.6200	-122.3980
Colorado Springs, CO	93037	38.8100	-104.6884
Washington, DC	13743	38.8650	-77.0340
Jacksonville, FL	13889	30.4940	-81.6930
Miami, FL	12839	25.8240	-80.3000
Atlanta, GA	13874	33.6400	-84.4270
Des Moines, IA	14933	41.5380	-93.6660
Boise, ID	24131	43.5650	-116.2200
Chicago, IL	94846	41.9860	-87.9140
New Orleans, LA	12916	29.9969	-90.2775
Portland, ME	14764	43.6422	-70.3040
Minneapolis, MN	14922	44.8830	-93.2290
Fargo, ND	14914v	46.9250	-96.8110
Portland, OR	24229	45.5910	-122.6000
Pittsburg, PA	94823	40.5010	-80.2310
Rapid City, SD	24090	44.0460	-103.0540
Memphis, TN	13893	35.0610	-89.9850
Dallas, TX	03927	32.8960	-97.0410
El Paso, TX	23044	31.8110	-106.3760
Lubbock, TX	23042a	33.6955	-102.0988
Salt Lake City, UT	24127a	40.8260	-112.1541
Seattle, WA	24233	47.4610	-122.3140
Spokane, WA	24157	47.6210	-117.5280
Rock Springs, WY	24027	41.5940	-109.0650

TASK THREE. Translate Projections into Relevant Indicators and Products

The first objective of this third task was to translate the high-resolution projections generated in Task 2 into climate indicators relevant to Southern Plains infrastructure. The second was to summarize this information in a limited number of data files, graphics, maps, and other products such as, for example, the projected changes in the temperature of the hottest day of the year or cumulative seasonal precipitation.

The secondary indicators were decided based on the extensive literature review and the survey described in Task 1. They were generated in netCDF format (though they will be available for download from ESRI in various user-friendly forms) and used to generate a series of regional maps examples of which are shown in Figure 1 for mean and 90th percentile statistics of seasonal cumulative precipitation.

TASK FOUR. Generate Final Data and Graphics Products

The final task in this project was to generate the final products and deliverables. The deliverables include the maps in Figure 1 (example of a graphic product, here showing the winter (December – February) and summer (May – September) mean and 90th percentile for seasonal total precipitation for 1980-2009 and the projected 90th percentile seasonal total precipitation for mid- and end-of-century for the higher RCP8.5 scenario CMIP5 model ensemble), the data that will be hosted online by ESRI, and data provided to collaborators for the modeling and infrastructure resilience assessments currently being undertaken by Drs. S. Senadheera, D. James, and D. Liang.

The analysis section, below, describes how the daily and hourly climate projections were generated to be used as input to the AASHTOWare Pavement ME Design™ model to simulate pavement performance and changes in lifetimes, modelled by Dr. Stoner for 25 stations across the U.S., as well as in the heat transfer model used by Dr. Athukorallage for Lubbock, TX, to model thermal performance of a typical asphalt system, the final steps in this task.

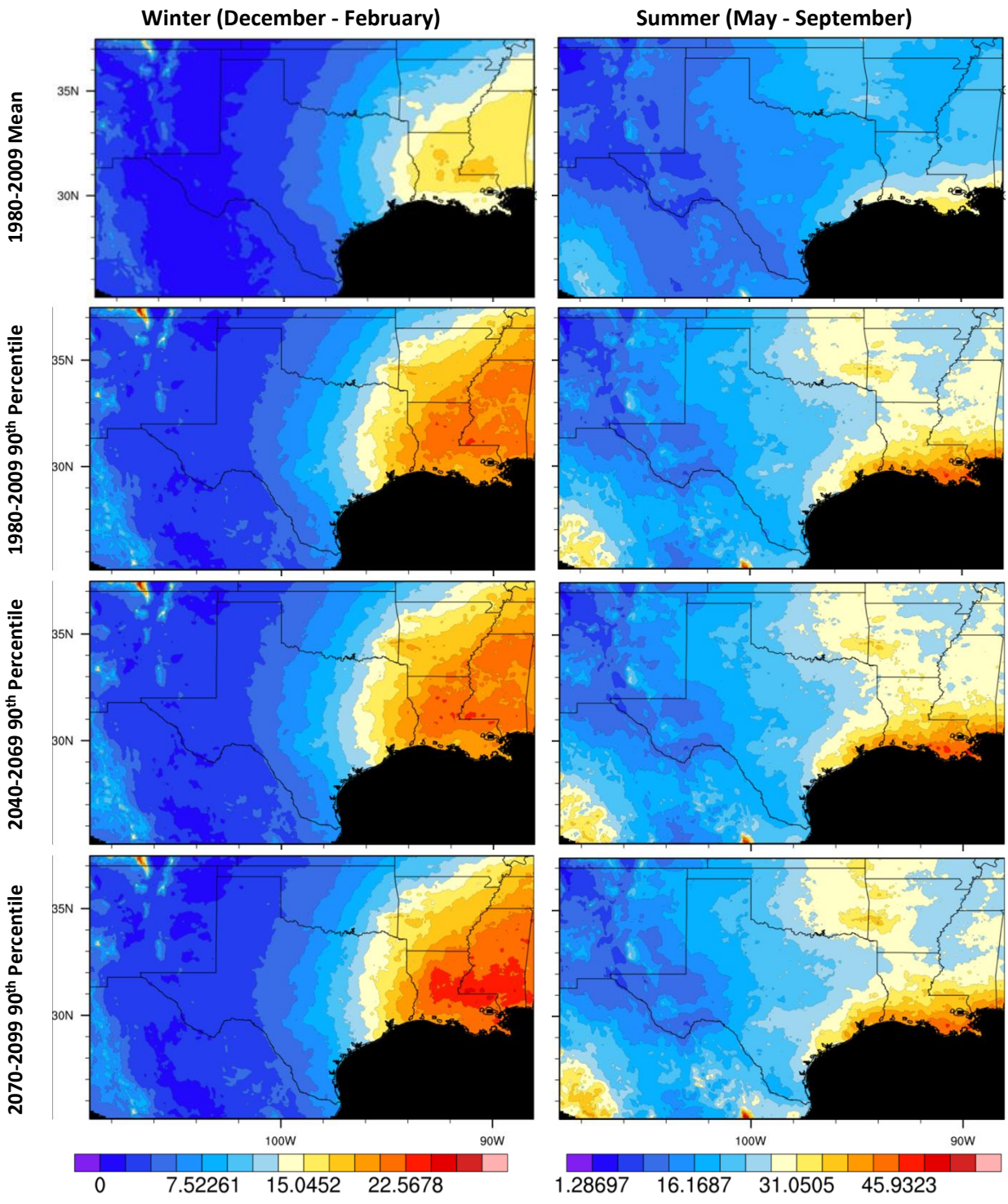

Figure 1. Examples of gridded regional products (see text above for figure details).

ANALYSIS

The temperature and precipitation data for the 25 daily station records across the country, described in Task 2 above, were disaggregated into hourly values by creating a 24-hour by 365-day surface from the 37 years of hourly observation data. Next, the surface was smoothed, interpolating it over the full range of daily minimum and maximum values, before applying it to the downscaled daily values to determine appropriate hourly conditions for that day of year and location. Daily total precipitation amounts were disaggregated to hourly values using a variation of the original methodology described in Socolofsky et al. 2001, which randomly separates the daily amount of precipitation into individual storm events. The number of storms allowed to occur per day were limited by binning the historical daily total rainfall into eight quantiles by rainfall amount, while keeping track of how many storms occurred per day. A maximum number of allowed rainfall events per day was assigned by randomly sampling from the number of events per day from the bin that encompassed the future daily total rainfall amount. Start and end times were randomly selected, while constraining each storm to begin and end within a 24-hour period. Rainfall from overlapping storms was added. Hourly wind speed and percent sunshine values were generated by randomly sampling a day (24 hourly values) in the historical data with similar daily total rainfall amount and that occurred in a three-month season surrounding the day in question. For example, if March 5, 2020, had a projected total rainfall amount of 0.6 inches, a day in the historical data between the months of February to April with a similar amount of total daily rainfall (within 0.25 inches), was randomly selected, and that day's 24-hour wind speed and percent sunshine was used for March 5, 2020. If no historical day existed with rainfall within 0.25 inches of the future daily rainfall, then the day with the closest daily rainfall amount was selected. For days with no rainfall, wind speed and percent sunshine were estimated by randomly sampling from those days with no rainfall during the three-month historical time period.

The hourly disaggregated climate variables were used as input to two separate analyses of the effect of climate change on pavement. The first analysis applied the American Association of State Highway and Transportation Officials (AASHTO) AASHTOWare Pavement ME Design™

pavement model to analyze the impact of potential future climate change on the performance and lifetime of asphalt pavement at 25 locations across the U.S. The historical and future climate simulations were used, in combination with information about the local subgrade and current suggested pavement performance grade binders, to evaluate the distress and time before failure thresholds are reached for two different types of flexible pavement: a relatively thick pavement, representative of typical interstate highways, and a thinner pavement, which represents a typical primary road. The model predicted performance of each of these pavement types were analyzed for three future periods (2001-2020, 2041-2060, and 2081-2100) for the higher RCP8.5 scenario and the GFDL-ESM2G climate model. The second analysis examined the variation heat transfer of an asphalt-concrete pavement structure for the warmest day of the year at a location in Lubbock, TX (Latitude: 33.5647, Longitude: -101.8778) for three time periods (1981-2000, 2041-4060, and 2081-2100) for the same climate model and scenario as the first analysis. The two sections below describe each of these analyses in more detail.

Projected changes to pavement performance and lifetimes

Four measures of pavement distress were analyzed for each of the pavement designs: asphalt concrete (AC) permanent deformation, total pavement permanent deformation, and international roughness index (IRI) for all sections, top-down fatigue cracking for the interstate sections and bottom-up fatigue cracking for the primary road sections. Top-down and bottom-up fatigue cracking are typically the dominant fatigue modes in interstate and primary road pavements, respectively, and therefore chosen for analysis in this study. The change number of months to reach failure thresholds for each distress at 98% reliability level were also examined. All values, except months to failure, are the terminal values at the end of the 20-year design.

Figures 2 and 3 show projected changes in performance between each of the three 21st century periods relative to the baseline period. Locations are sorted by their degree of projected increase in daily maximum temperature (shown as red dots) between the baseline and the end-of-century period average, as simulated by downscaled projections from the GFDL-ESM2G GCM under the higher RCP8.5 scenario described above. Projected increases in daily maximum temperature by end-of-century range from the smallest increase of 5.7°F in Portland, ME, a

coastal city where changes in climate are moderated by cooler ocean temperatures, to the proportionally greatest increase of 10.8°F in Boise, ID, an inland, northern location expected to experience more warming than coastal locations and those further south. Add a sentence here talking about cities in our region.

Interstate Pavement

Results from the analysis of interstate pavement simulations indicate that for nearly all sites, periods, and types of distress, pavement performance is reduced in future time periods compared to the baseline period (1981-2000), and this reduction increases under greater amounts of change (Figure 2).

For the earlier period (2001-2020), increases in AC permanent deformation (Figure 2a, dark bars) range between 0 and 0.05 inches. Mid-century (2041-2060; medium gray bars) values range between 0.02 and 0.08 inches, and end-of-century (2081-2100; light gray bars) values are between 0.08 and 0.18 inches. Total permanent deformation values (Figure 2b) increase in all locations and periods, except for El Paso, TX, in the early period, which sees no change from the baseline values. The ranges are identical to those for AC permanent deformation, except for the end-of-century simulations where the values range between 0.07 and 0.18 inches. Overall, AC and total permanent deformation results show similar performance to one another for the interstate pavement, with a slight increase in deformation values for both the early- and mid-century simulations, followed by a larger increase toward the end of the century, indicating that for all locations the pavement rapidly deteriorates when the ambient temperature regularly exceeds the performance grade temperature range it is designed for.

Nearly all locations show increases in AC top-down fatigue cracking that increase towards the end of the century (Figure 2c). Early-century increases in top-down fatigue cracking range from -5.3 to 179.9 feet per mile relative to the baseline period, mid-century increases range between 29.0 and 229.1 feet per mile, and by the end of the century the projected increases range between 62.5 and 513.5 feet per mile. Although trends point toward increased AC top-down fatigue cracking toward the end of the century, there is no clear correlation between the

amount of change at the end of the century and the amount of warming projected at that location.

Bottom-up fatigue cracking (not pictured) is also important for thicker pavements, such as interstate pavements. Results show that the changes in bottom-up cracking, resulting from a warmer climate, were in all locations and future scenarios less than 0.04% increase, indicating that climate change does not significantly impact bottom-up fatigue cracking in interstate pavements.

Terminal IRI also increases in nearly all locations and for all periods (Figure 2d), with changes for the early period ranging between -0.32 to 2.79 inches per mile. Four sites (Des Moines, IA; El Paso, TX; Dallas/Fort Worth, TX; and New Orleans, LA) experience a slight decrease from the baseline period, followed by an increase in the two later periods. For the mid-century period, the change in terminal IRI values range between 0.04 and 3.48 inches per mile; however, not all locations experience an increase from the earlier period, indicating that for those locations IRI is not as affected by changes in climate between the early and middle of the century. The end-of-century period for many locations show a drastic increase in IRI compared to the baseline period, with increases ranging between -0.46 and 7.75 inches per mile. The only negative value is for Seattle, WA, which shows a small increase in IRI in the early period but then a decrease in the middle and end-of-century periods. Portland, OR, shows similar traits for changes in IRI for the interstate pavement design.

For the end-of-century simulations there appears to be a strong correlation between both AC and total permanent deformation and the projected end-of-century increase in temperature. Some correlation with changes in temperature is visible in terminal IRI values, but less so in top-down fatigue cracking, although there are still increases in many locations, indicating that other factors such as changes in moisture could be more dominant than temperature.

Changes to the time it takes for pavement to reach its failure threshold provides a common measure to identify the relative impact of changes to failure modes. Figure 3 shows the change in number of months to reach the failure threshold for the interstate pavement for each of the

four measures of performance under each of the three future periods. At 98% reliability, the failure thresholds were 0.25 inches for AC permanent deformation, 0.75 inches for total pavement permanent deformation, 2000 feet per mile for AC top-down fatigue cracking, and 172 inches per mile for IRI. Missing bars for a location mean that the pavement did not fail for that parameter during the 20-year baseline period and therefore no comparison is possible for the remaining periods.

Climate change strongly impacts AC permanent deformation (Figure 3a). As temperature increases across most sites, it decreases the time to when the failure threshold is reached. The largest decrease is for the end-of-century period in Seattle, WA, with failing occurring two years earlier in the near future and almost five years earlier by the end of the century.

Of the four performance measures, total permanent deformation (Figure 3b) has the largest decreases in time to failure, although five locations, four of them in the northern part of the continental U.S. and one in a cooler coastal climate, do not fail during the 20-year baseline period (Chicago, IL; San Francisco, CA; Seattle, WA; Portland, OR; and Portland, ME). Boise, ID shows the largest decline in time to failure, with a decrease of 94 months; in other words, failing almost eight years earlier by end of century relative to the baseline period. Many other locations see similar large decreases in performance for the later period and even the cooler coastal climate sites that did not fail for total pavement permanent deformation during the baseline period have significant AC permanent deformation.

Top-down fatigue cracking (Figure 3c) does not cause failure of the interstate pavement for many of the locations during the baseline period. Of the sites that do fail, the deterioration due to top-down fatigue cracking is more important than AC permanent deformation. For example, Boise, ID is already seeing considerable changes in the time to reach failure due to top-down fatigue cracking, and is anticipated to fail up to seven years earlier from top-down fatigue cracking as compared to two years earlier from AC permanent deformation towards the end of century. For IRI (Figure 3d), seven sites do not fail during the baseline period: El Paso, TX; San Francisco, CA; Seattle, WA; Portland, OR; Miami, FL; Jacksonville, FL; and Portland, ME, which all

are southern and coastal sites. Of the sites that do fail, only modest decreases in the time to failure are anticipated for IRI.

While increasing temperature typically decreases the time it takes for the pavement to reach the failure threshold, changes in months to failure for these four measures of pavement distress are not well correlated to changes in daily maximum temperature at the end of the century (red dots). There are also no obvious correlations between sites in the same LTPP climate zone and changes in performance measures. These results suggest that site-specific analyses that include both projections of climate change and pavement analyses are essential to understand how pavement distress will be impacted by a changing climate.

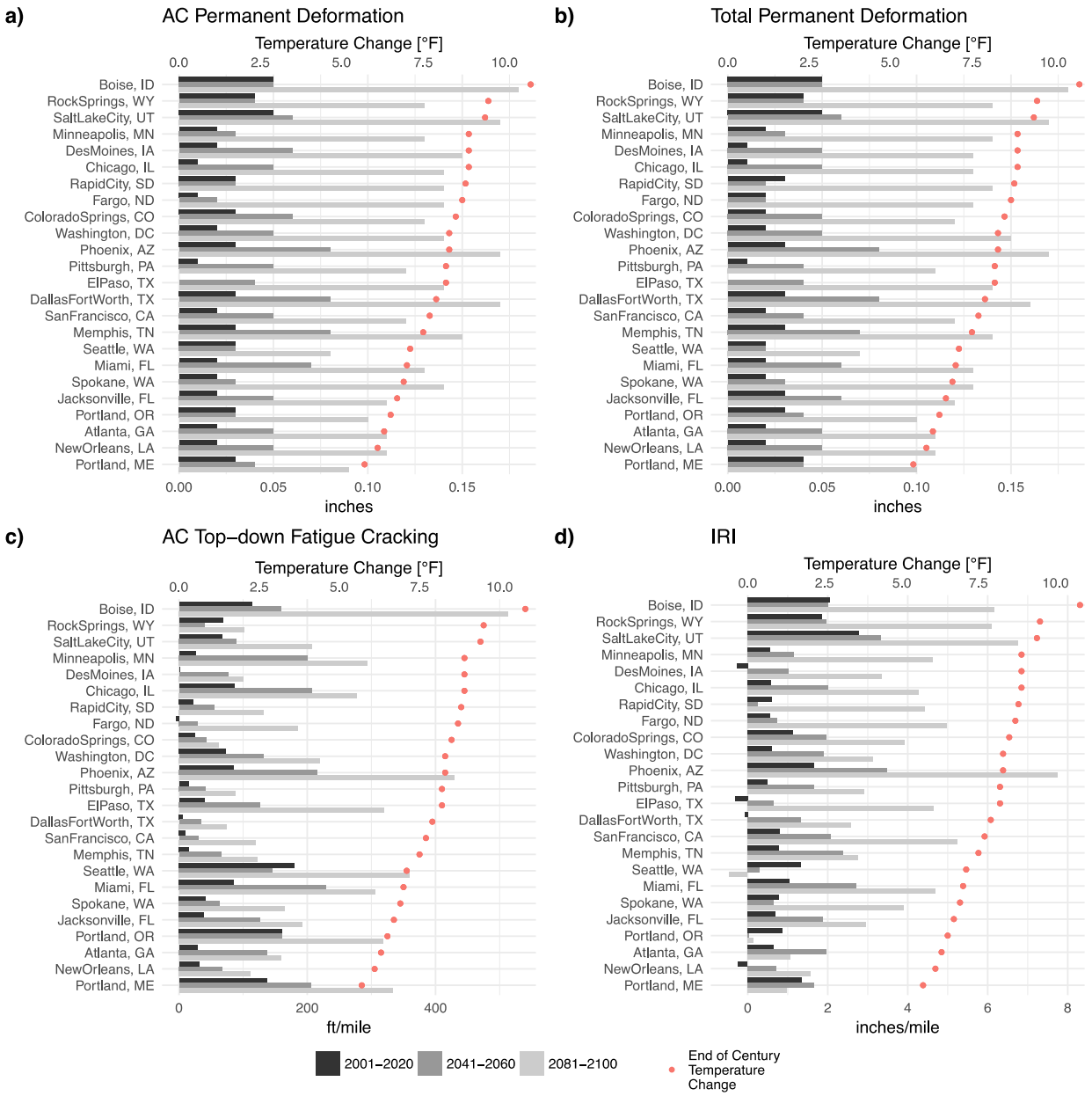

Figure 2. Projected changes in terminal distress values for interstate pavement.

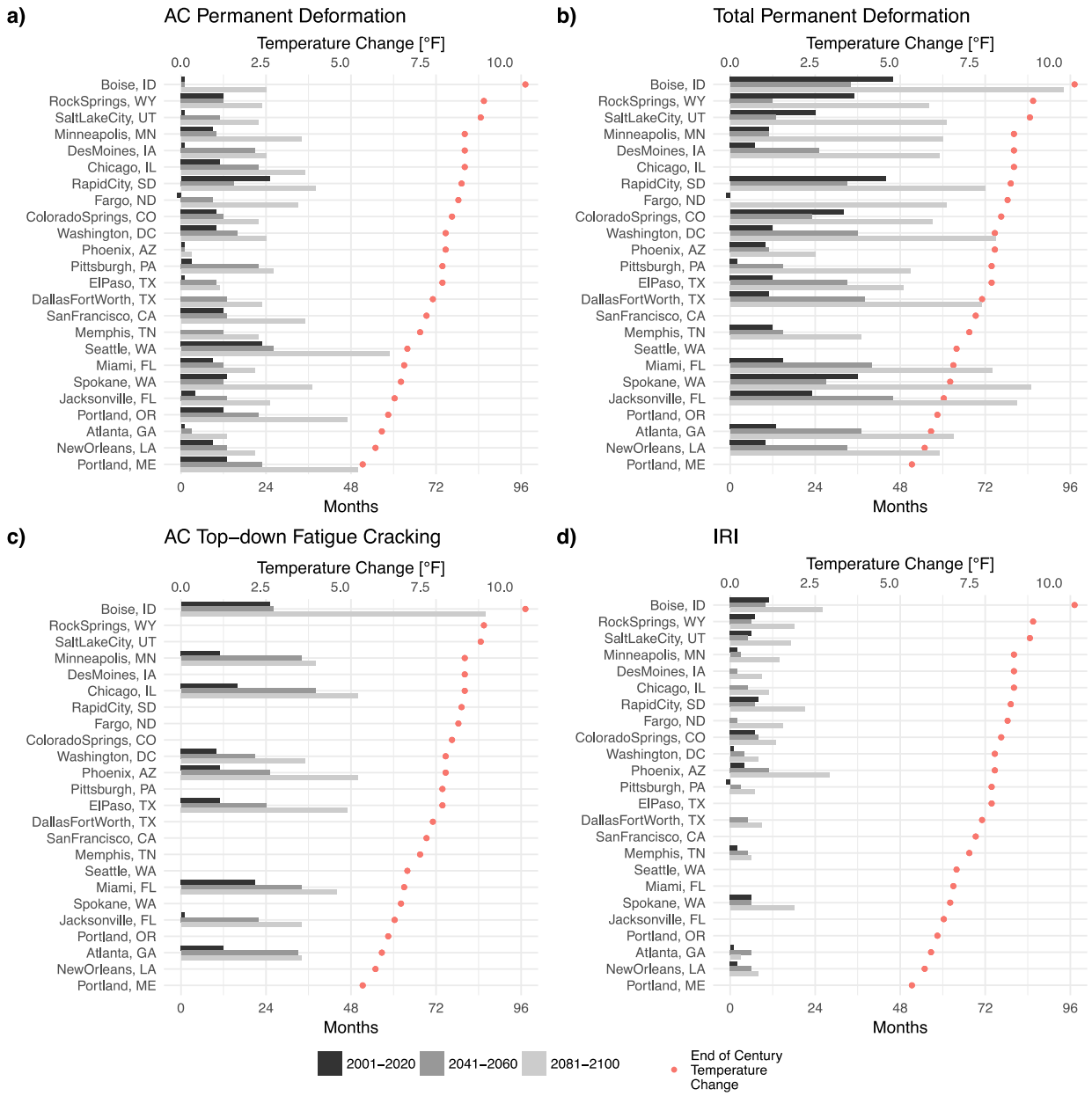

Figure 3. Change in number of months for interstate pavement to reach failure.

Primary Road Pavement

Similar to interstate pavement design, the results for primary road design show decreased performance in many of the locations under a warmer climate. Climate change clearly affects primary road AC permanent deformation (Figure 4a), with increases at all locations for nearly all periods. For the early period, increases in AC permanent deformation from the baseline

period range between 0 and 0.04 inches though two locations, Pittsburgh, PA, and El Paso, TX, do not see any changes. For the mid-century period, increases are between 0.02 and 0.06 inches, whereas the end-of-century period has larger increases from 0.06 to 0.14 inches. Generally, northern sites see higher increases in AC permanent deformation compared to more southern locations. Add a sentence here talking about our region

The results also show decreased performance with respect to total permanent deformation (Figure 4b) for all three 21st century periods, as for the interstate pavement; the only exception is Fargo, ND, where during the first two periods there are small decreases in total permanent deformation (bars pointing to the left), relative to the base period, but then a larger increase for the last, and warmest, period. During the early- and mid-century periods, total permanent deformation changes from the baseline period range between -0.01 and 0.05 inches and -0.01 to 0.06 inches, respectively, whereas in the later period they increase to between 0.06 and 0.14 inches. Similar to interstate pavements, there is a strong positive correlation between the later period increases in deformation and the end-of-century daily maximum temperature increases relative to the baseline period. For many locations the change in permanent deformation, both total and AC, is almost exponential, i.e. close to a doubling for each future period, emphasizing the importance of changing the pavement binder grade as temperatures warm.

Bottom-up fatigue cracking (Figure 4c) for the thinner primary road pavements seems to be less affected by changes in climate. Only a few locations show a consistent increase in cracking as temperature increases. The changes in percentage points from the baseline period are very small, ranging between -0.36 and 1.06% for the early period, between -0.28 and 2.1% for the mid-century period, and from -0.65 to 3.91% for the later period. El Paso, TX, and Phoenix, AZ, both hot and dry climates in the “dry-nonfreeze” climate zone, are the only sites with a significant trend and larger increases in bottom-up fatigue cracking, indicating that the southwest may be an area where more focus should be placed on this measure of distress. There appears to be no correlation between bottom-up fatigue cracking at the end of the century and changes in daily maximum temperature for the same period. Mention something about our region here too

Many locations show increases in IRI (Figure 4d) under the three future climates for the primary road pavement, although several locations show decreases. For example, Seattle, WA again appears as an area where values of IRI improve under a warmer climate. For the early period, IRI values relative to the baseline period range from -0.87 to 2.6 inches per mile; for the mid-century period, values range between -0.52 and 2.81 inches per mile; and for the end-of-century period they range between -1.33 and 6.26 inches per mile. The largest decrease relative to the baseline is for the later period in Seattle, WA, and the largest increase is for Phoenix, AZ. There does not appear to be any regional trends in IRI and also no direct correlation with the increase in temperature at the end of the century. Talk about our region again

For the primary road pavement, at 98% reliability, the failure thresholds were 0.25 inches for AC permanent deformation, 0.75 inches for total pavement permanent deformation, 25% lane area for AC bottom-up fatigue cracking, and 172 inches per mile for IRI. Results for AC permanent deformation (Figure 5a) show relatively large decreases in the time it takes the primary road pavement to reach the failure threshold. Only Seattle, WA, does not reach the failure threshold for the baseline period, and changes for the remaining periods therefore do not show up in the figure. The largest projected decrease is for Portland, ME, which, at the end of the century sees a reduction in the time it takes to reach the pavement failure threshold of 96 months, or eight years, based on AC permanent deformation alone. And here too

For total permanent deformation (Figure 5b), there are also clear changes in the number of months to failure. Three locations do not fail during the baseline period (Seattle, WA; Portland, OR; and Portland, ME), but for the majority of the remaining locations, there is a significant trend, with Boise, ID, showing the largest change of 75 months, or over six years' decrease in the time it takes the pavement to reach the failure threshold relative to the baseline period. Fargo, ND shows an increase of almost a year to the failure threshold is reached for the two later periods, as one of the only locations analyzed here with an improvement to the pavement performance as the climate warms. And here

AC bottom-up fatigue cracking (Figure 5c) shows slight decreases in the months to failure for most of the locations. El Paso, TX, and Phoenix, AZ, do not stand out here as they did when

examining the absolute values. El Paso is also the only location that does not fail for this measure during the baseline period. A few locations show an increased performance (bars pointing to the left) as the climate warms. AC bottom-up fatigue cracking does not appear to be as affected by a warming climate, with the largest decrease in months to the failure threshold is reached at the end of the century being 18 months for Portland, OR.

For IRI (Figure 5d) there is not a significant change for the majority of the locations, relative the baseline period. Three of the locations do not fail for IRI during the baseline period (El Paso, TX; Seattle, WA; and Miami, FL). Phoenix, AZ, is again the location with the largest decrease in months until failure, with a reduction of 22 months before the pavement fails according to the IRI threshold and reliability level.

Similar to the interstate pavement, there does not appear to be obvious correlations between changes in months to failure for the four measures of pavement distress, and changes in daily maximum temperature at the end of the century. For locations {which ones?} in the Southern Plains, … summarize the findings.

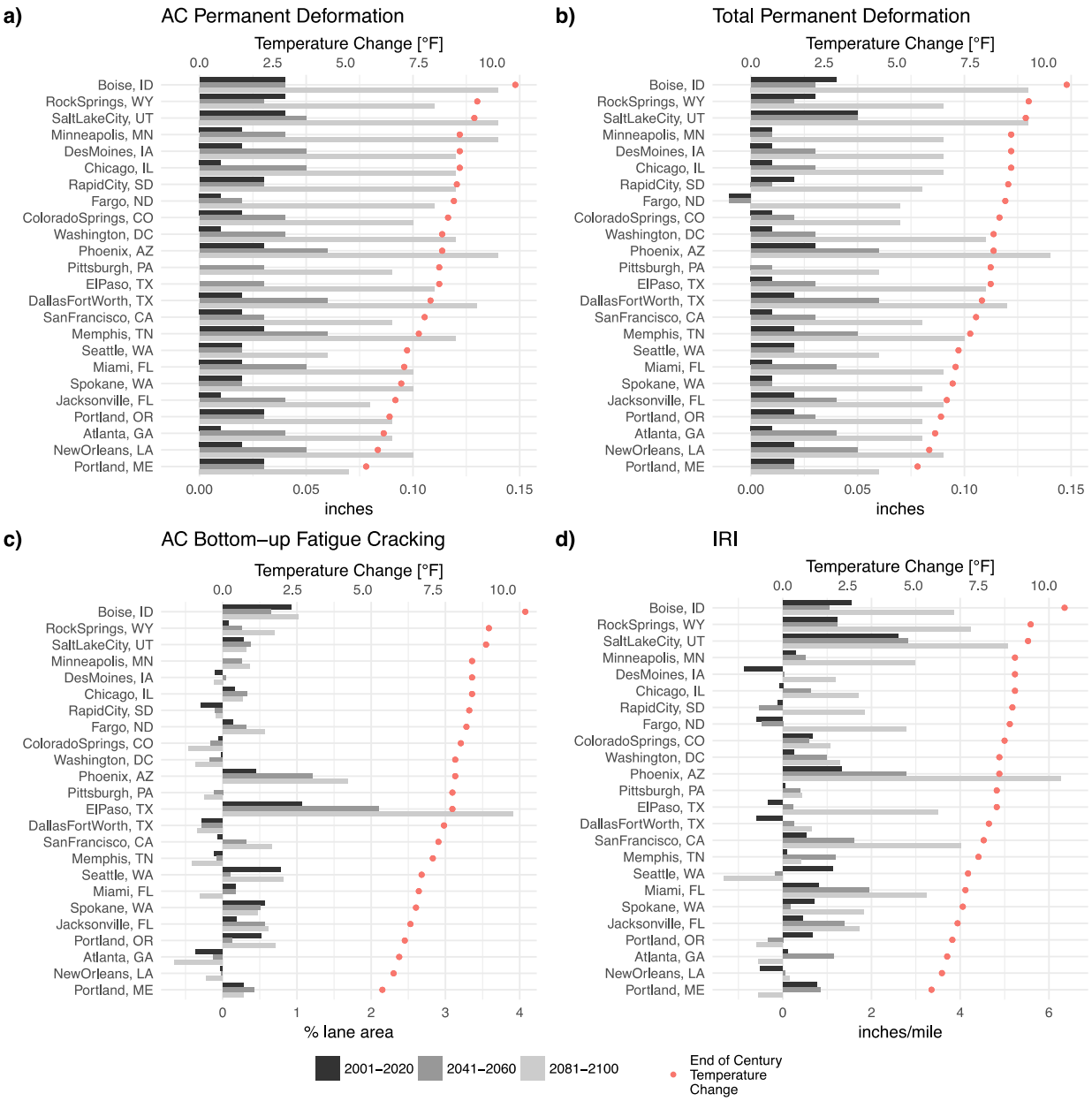

Figure 4. Projected changes in terminal distress values for primary road pavement.

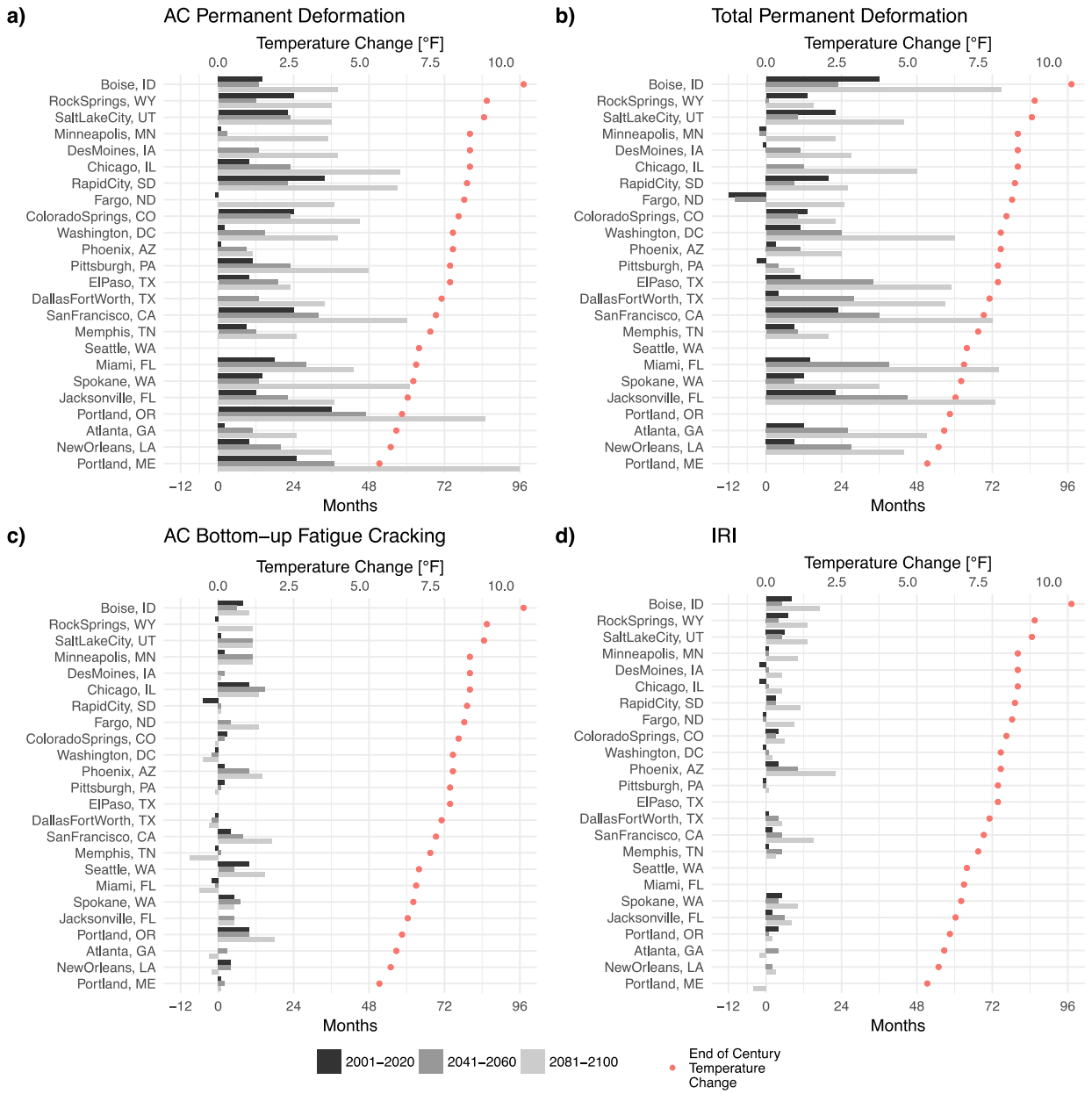

Figure 5. Change in number of months for primary road pavement to reach failure.

Heat transfer modeling through flexible pavement

In this second analysis, our main goal is to examine the variation of the maximum surface temperature of an ac-pavement structure for the warmest day of the year in Lubbock-TX (Latitude: 33.5647 Longitude: -101.8778) for three time periods: 1981-2000, 2041-2060, and

2081-2100. The simulations are performed utilizing the 24-hour ambient temperature, solar radiation, and relative humidity data corresponding to the three time periods.

Modeling equations, boundary and initial conditions

We consider a multilayered semi-infinite pavement geometry that consists of three layers: asphalt-concrete layer, base layer, and subbase layer. A schematic diagram of the cross-sectional view of the pavement system is shown in Figure 6. The thickness of each layer is: asphalt-concrete layer–t_{ac}, base layer–t_{base}, and subbase layer–t_{s-base}, respectively. Let the origin of the Cartesian coordinates system be at the middle of the outer surface of the asphalt-concrete layer (see Figure 6) and let $y_0 = 0$ and$y_b = t_{ac} + t_{base} + t_{s-base}$. As considered in previous research (Athukorallage, et al. 2018), we assume constant thermophysical properties in each of the pavement layers. k_i, c_{pi}, and ρ_i are the thermal conductivity, specific heat capacity, and the density of the material contained in the i^{th} pavement layer, respectively.

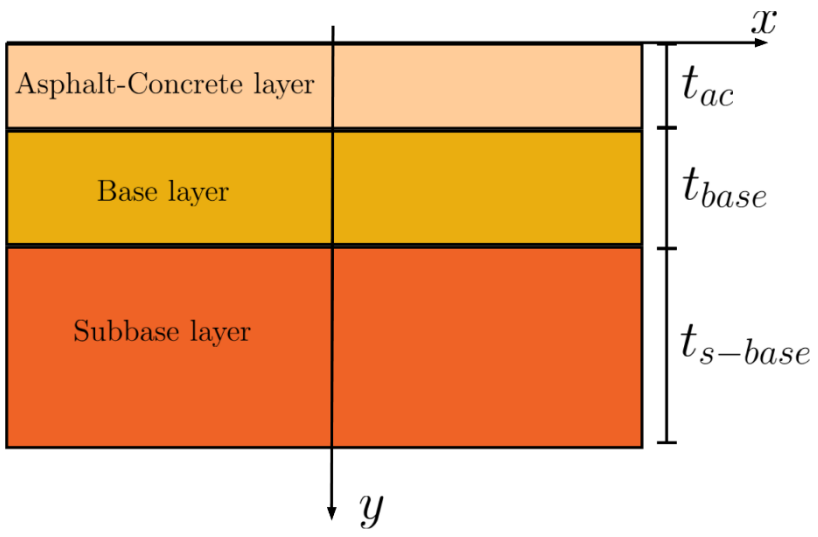

Figure 6. Cross-sectional schematic of an asphalt-concrete pavement system.

The temperature variation, $T(x, y, t)$, in a layer i is obtained by solving the transient heat equation:

$$\rho_i \, c_{p,i} \frac{\partial T_i}{\partial t} = \nabla \cdot (k_i \nabla T_i) \quad \forall (x, y) \in (-\infty, \infty) \times [y_{i-1}, y_i] \text{ and } t > 0, \qquad (1)$$

with the appropriate boundary and initial conditions. These boundary and initial conditions mainly depend on incoming and outgoing solar radiation, ambient and sky temperatures, and thermophysical properties of the asphalt-concrete layer.

Initial and boundary conditions

We assume the pavement surface (that is $y = 0$) is subjected to time-dependent solar flux, convective and radiative heat fluxes. As illustrated in Figure 7, suppose the pavement surface is exposed to a time-varying *direct normal solar radiation* $\dot{Q}(t)$, heat transfer rate due to convection and radiation $\dot{Q}_{conv}(t)$ and $\dot{Q}_{rad}(t)$, respectively, and air temperature $T_{\text{air}}(t)$.

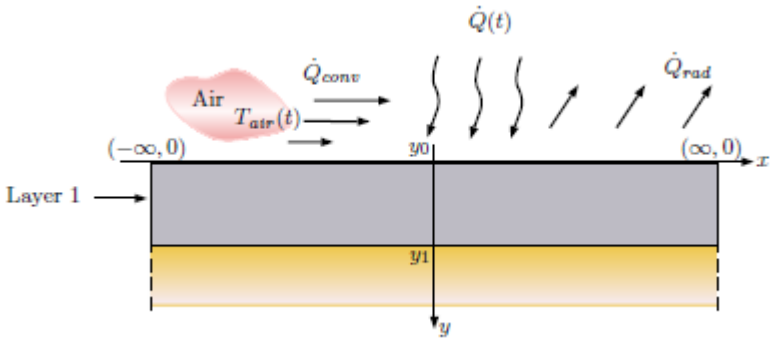

Figure 7. Surface energy balance at y =0.

Then considering the net heat transfer at the pavement surface, we obtain:

$$k_{ac} \nabla T_s = \alpha_{ac} \dot{Q}(t) - h_c \big(T_s - T_{amb}(t)\big) - \epsilon_{ac} \sigma \left(T_s^4 - T_{sky}^4(t)\right), \qquad (2)$$

where, T_s is the pavement surface temperature, h_c denotes the convective heat transfer coefficient, α_{ac} and ϵ_{ac} are the absorptivity and emissivity of the pavement surface, and σ

denotes the Stefan-Boltzmann constant. Moreover, $T_{amb}(t)$ and $T_{sky}(t)$ are the air and sky temperatures. In equation (2), the terms in the right side denote the solar energy absorbed by the surface, convective heat transfer occurring at the pavement surface, and the outgoing radiation heat transfer from the surface, respectively. In addition, the initial temperature T_{ini} and the temperature at bottom of the subbase T_{bot} are taken to be a constant with $T_{ini} = T_{bot}$.

Numerical results

In the following simulation studies, our main goal is to examine the variation of the maximum surface temperature of an ac-pavement structure for the warmest day of the year in Lubbock-TX (Latitude: 33.5647 Longitude: -101.8778) for three time periods: 1981-2000, 2041-2060, and 2081-2100. The simulations are performed utilizing the 24-hour ambient temperature, solar radiation, and relative humidity data corresponding to the three time periods. Note that the surface boundary condition, equation (2), contains the sky temperature, $T_{sky}(t)$ as a variable parameter expressed as (Gui, et al. 2007).

$$T_{sky} = T_{amb}(0.004T_{dew} + 0.8)^{0.25}. \quad (3)$$

In equation (3), the dew-point temperature, T_{dew}, is calculated using the model (Gui, et al. 2007).

$$T_{dew} = 0.1T_{amb} - 112 + \left(\frac{RH}{100}\right)^{\frac{1}{8}}(112 + 0.9T_{amb}), \quad (4)$$

where RH denotes the relative humidity expressed as a percentage. Figure 8 illustrates the predicted air temperature and solar radiation for the warmest day in year 2000. The fixed parameters and thermophysical properties used in the simulations are given in Tables 2 and 3. Figure 9 shows the solar radiation, air temperature, and relative humidity profiles corresponding to the three time periods considered in the study.

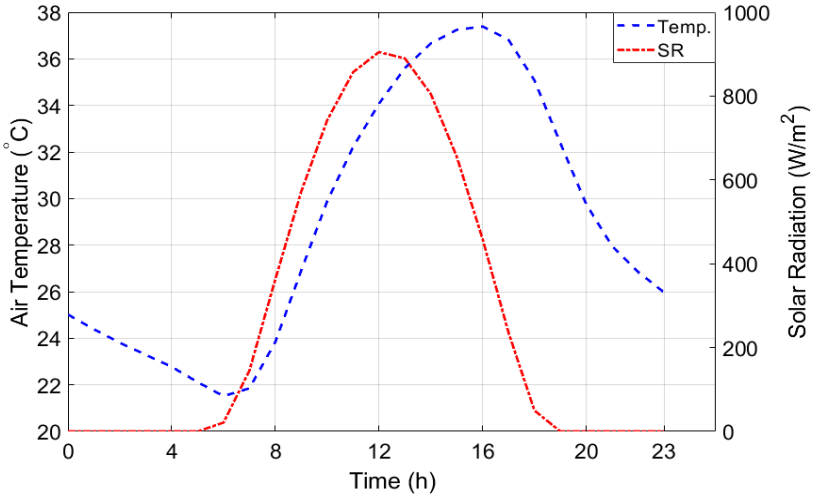

Figure 8. Air temperature and solar radiation profile for the hottest day in year 2000.

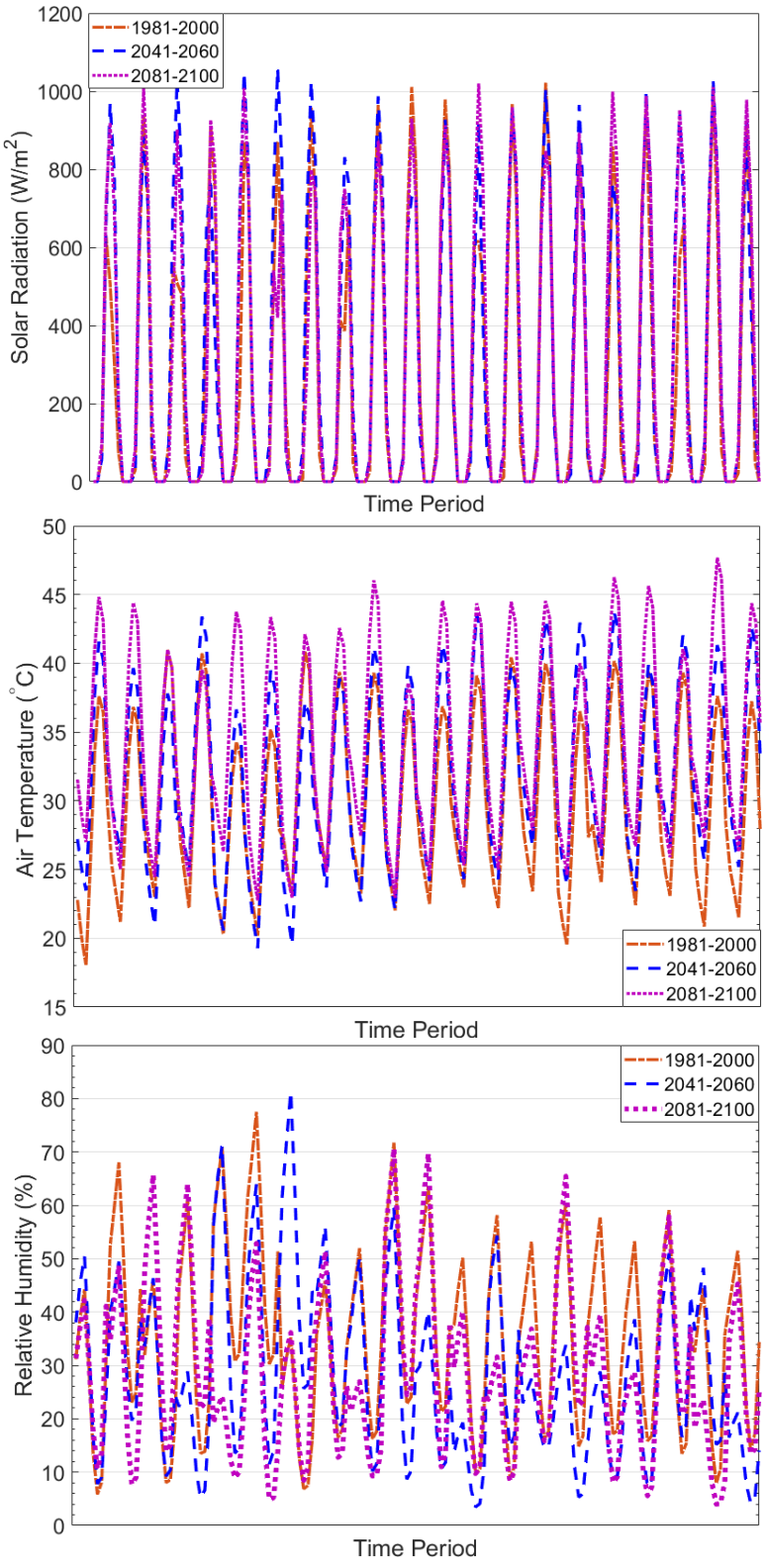

Figure 9. Solar radiation, air temperature, and relative humidity profiles.

Table 2. Thermophysical properties of pavement layers.

Layer	Density ρ (kg/m^3)	Thermal conductivity k (W/(m · K))	Heat capacity c_p (J/(kg· K))	Thickness cm (in)
Asphalt-concrete	2300	1.83	920	10.2 (4)
Base	1950	1.83	1100	15.2 (6)
Subbase	1925	1.80	900	20.3 (8)

Table 3. Fixed parameter values.

Parameter	Value	Unit
h_c	20	W/(m^2 · K)
α_{ac}	0.9	–
ε_{ac}	0.9	–

The temperature variation of the pavement surface is obtained by solving equation (1) subject to the boundary condition given in equation (2).

The initial temperature of the pavement structure is taken equal to the air temperature at time $t = 0$. Next, we perform simulations to study the surface temperature variation for the three time periods considered, and a simulated pavement surface temperature profile that corresponds to year 2000 is given in Figure **Error! Reference source not found.**10. It can be observed that the minimum pavement temperature occurs during the early morning and surface temperature gradually increases as a result of the incoming solar radiation. Further, the maximum surface temperature approximately equals to 52.1°C.

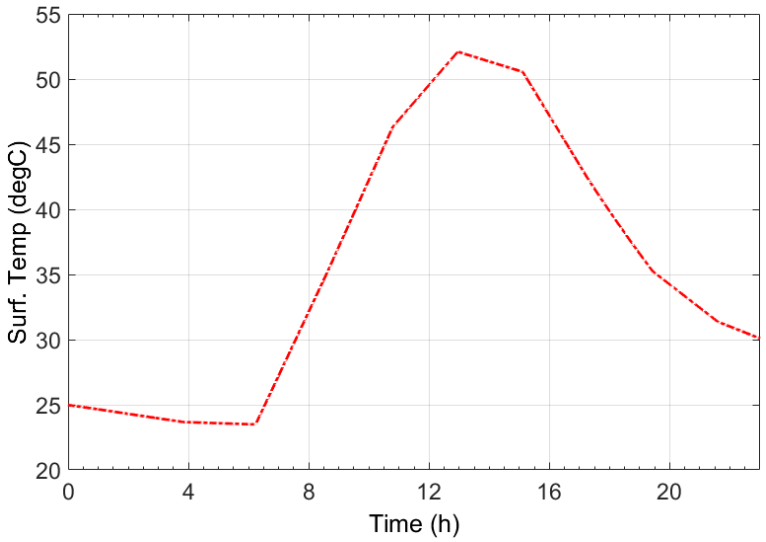

Figure 10. Calculated pavement surface temperature variation for the hottest day in year 2000.

Figure 11 shows the maximum surface temperature values for the warmest day of the year for the three time periods: 1981-2000, 2041-2060, 2081-2100. Here, for the three time periods considered, the maximum temperature varies between [44.6, 57.4], [51.8, 60.1], and [50.4, 62.6], respectively. Furthermore, the corresponding average temperatures are 52.1, 56.1, and 57.9°C. The largest maximum surface temperature for the period of time considered occurs in 2099, and interestingly, it corresponds to the year with the highest air temperature though not the highest solar flux.

In general, the figure clearly shows an increase in the maximum surface temperature for the two future-time periods. However, in the current analysis, each simulation utilizes the data that corresponds to a single day, and hence, we are unable to observe the impact of heat accumulation in the pavement system on its temperature. Moreover, the surface boundary condition depends on the combined effects of many parameters, such as the ambient temperature, solar radiation, relative humidity, wind velocity, and cloud cover. Hence, there can be days resulting in high pavement temperature values. Therefore, we are planning to perform more analyses over a longer time period to observe more definitive conclusions.

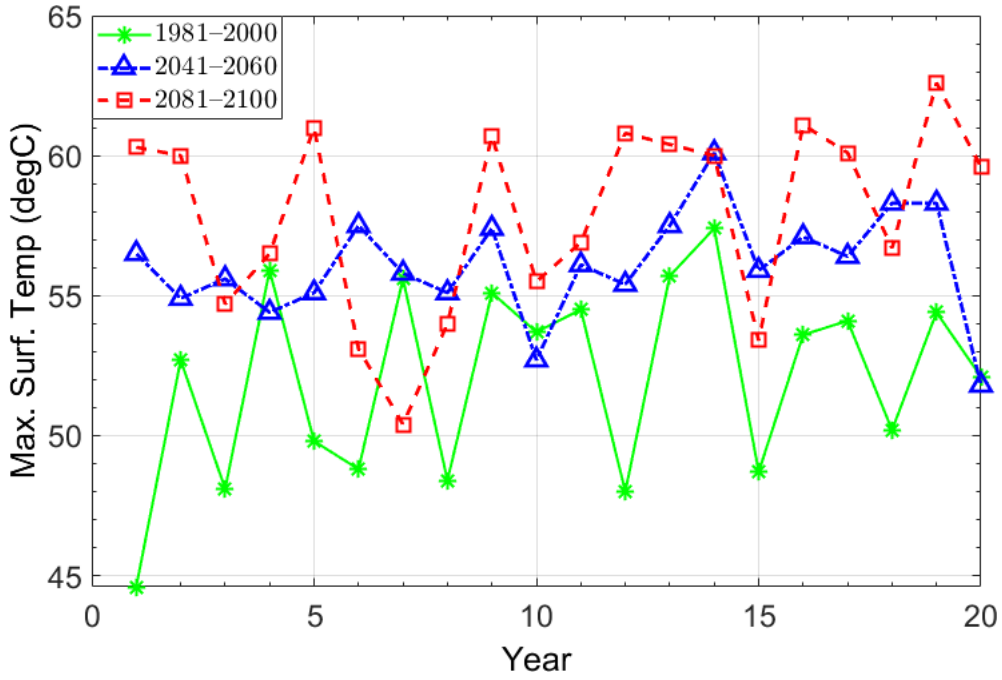

Figure 11. Maximum pavement surface temperature for the warmest day of the year.

DISCUSSION

The results indicate that increasing temperatures have a negative effect on both interstate and primary road flexible pavements for the majority of the locations included, especially for measures of permanent deformation, or rutting, which is more pronounced under warmer temperatures (see Figures 2 - 5), echoing the findings of others (Mills et al., 2009 and Meagher et al., 2012). Locations in the Southern Plains show significant increases in permanent deformation, where warming temperatures cause the asphalt material to soften, increasing the potential for rutting, which in return results in lower expected lifetime of the pavement, with the time when metrics of failure is reached happening between four to six years earlier than observed presently.

For interstate pavements, results show increases in the amount of AC top-down fatigue cracking as the climate warms, however there does not appear to be any direct correlation to the amount of warming at the end of the century. For primary roads there is no clear

relationship between the change in AC bottom-up fatigue cracking and changes in warming, except for very hot and dry locations in the Southern U.S., such as Phoenix, AZ, and El Paso, TX, which both showed an increasing trend toward the end of the century. Increases in IRI are also expected for both types of pavement, with the largest increases expected for Phoenix, AZ, for both types of pavements.

Increases in end-of-century asphalt concrete and total permanent deformation tend to be positively correlated with temperature increases; i.e. locations that are projected to experience more warming also have the largest increase in permanent deformation relative to the baseline period.

The flexible pavement thermal conductivity and surface temperature simulations for Lubbock, TX, shows that the farther we get into the 21st century, the hotter the pavement surface gets on the hottest day of the year, which is not surprising, and goes hand in hand with the results from the first pavement study, which projected more pronounced deformation earlier in the lifetime of the pavement due to hot temperatures in the Southern Plains as well as elsewhere in the continental U.S.

CONCLUSIONS

Modern infrastructure is designed and built to withstand historical variations in temperature, precipitation, and other aspects of weather. Today, however, the long-term statistics of historical climate are changing. Average temperature is increasing, precipitation is shifting, and many extremes, including heat waves and heavy precipitation events, are becoming stronger and more frequent. As a result, current pavement design based on historical conditions may not provide adequate durability in the future, as conditions exceed the range of those under which the pavement was designed to operate.

Flexible pavements are designed to perform optimally under certain temperature ranges and environmental conditions, with the performance grade, among other factors, determining the pavement durability under these varying conditions. The design performance grade therefore depends on the climate in the area where the road is being built. If the annual temperature

range in that region changes, these results show that in almost all regions of the continental U.S., the design of pavements must account for this before it happens or the pavement will experience a shorter lifespan and end up being costlier due to more frequent need for repairs and resurfacing.

The data generated and analyses conducted under this project quantifies projected changes in climate and their potential impact on pavement on different locations across the continental U.S. to give an overview of how climate change could impact pavement performance as well as changes in the time it takes the pavement to reach specified failure thresholds.

The unique results presented here indicate that increasing temperatures have a negative effect on flexible pavements for the majority of the locations included here for all measures of deformation as well as increases to the temperature gradient within the asphalt structure, which is more pronounced under warmer temperatures, echoing the findings of Mills et al. (*3*) and Meagher et al. (*4*). For pavement performance measures northern locations tend to show the largest increases in permanent deformation, where warming temperatures cause a reduction in the number of freeze days to be replaced by warmer days, increasing the potential for rutting. Increases in end-of-century AC and total permanent deformation tend to be positively correlated with temperature increases; i.e. locations that are projected to experience more warming also have the largest increase in permanent deformation relative to the baseline period.

Although these results present a broad overview of how climate could impact flexible pavement performance, more research is needed to understand how the changes in different climate variables cause the pavement performance to change. Studies are also needed to examine how individual changes in the pavement structure and materials may enhance the pavement performance. This could lead to understanding how individual locations might alter the design, materials, and performance grade binder to optimize the performance and lifetime of the pavement.

In addition, these results demonstrate how GCM output can be translated into the information required to simulate pavement performance and demonstrate that there is a risk if future climate conditions are ignored, and highlighting the critical importance of more research in this area. Studies such as these, along with the regional and national maps of specific indicators, should help guide infrastructure planners and designers when building new roads and other infrastructure to ensure it is build to withstand current and future warming trends.

REFERENCES

Athukorallage, B, Dissanayaka, T., Senadheera, S., and James, D. 2018. "Performance analysis of incorporating phase change materials in asphalt concrete pavements." *Construction and Building Materials* 164: 419-432.

Dixon, K.W., J.R. Lanzante, M.J. Nath, K. Hayhoe, A. Stoner, A. Radhakrishnan, V. Balaji, C.F. Gaitan, 2016. Evaluating the stationarity assumption in statistically downscaled climate projections: is past performance an indicator of future results? *Clim. Change*, 135, 395-408.

Gui, J., P. E. Phelan, K. E. Kaloush, and J. S. Golden. 2007. "Impact of pavement thermophysical properties on surface temperatures." *Journal of Materials in Civil Engineering* 19 (8): 683-690.Meagher, W., J.S. Daniel, J. Jacobs, and E. Linder. Method for Evaluating Implications of Climate Change for Design and Performance of Flexible Pavements. *Transportation Research Record: Journal of the Transportation Research Board*, 2012. 2305: 111-120.

IPCC, 2007: Climate Change 2007: Synthesis Report. Contribution of Working Groups I, II and III to the Fourth Assess- ment Report of the Intergovernmental Panel on Climate Change [Core Writing Team, Pachauri, R.K and Reisinger, A. (eds.)]. IPCC, Geneva, Switzerland, 104 pp.

IPCC, 2013: *Climate Change 2013: The Physical Science Basis. Contribution of Working Group I to the Fifth Assessment Report of the Intergovern- mental Panel on Climate Change* [Stocker, T.F., D. Qin, G.-K. Plattner, M. Tignor, S.K. Allen, J. Boschung, A. Nauels, Y. Xia,

V. Bex and P.M. Midgley (eds.)]. Cambridge University Press, Cambridge, United Kingdom and New York, NY, USA, 1535 pp.

Meagher, W., J.S. Daniel, J. Jacobs, and E. Linder. Method for Evaluating Implications of Climate Change for Design and Performance of Flexible Pavements. *Transportation Research Record: Journal of the Transportation Research Board*, 2012. 2305: 111-120.

Melillo, Jerry M., Terese (T.C.) Richmond, and Gary W. Yohe, Eds., 2014: *Climate Change Impacts in the United States: The Third National Climate Assessment*. U.S. Global Change Research Program, 841 pp. doi:10.7930/J0Z31WJ2.

Mills, B.N., S.L. Tighe, J. Andrey, J.T. Smith, and K. Huen. Climate Change Implications for Flexible Pavement Design and Performance in Southern Canada. *J. Transportation Engineering*, 2009. 135: 773-782.

Socolofsky, S., E.E. Adams, and D. Entekhabi. Disaggregation of Daily Rainfall for Continuous Watershed Modeling. *Journal of Hydrologic Engineering*, 2001. 6: 300-309. https://doi.org/10.1061/(ASCE)1084-0699(2001)6:4(300).

Stoner, A.M.K., K. Hayhoe, X. Yang, and D.J. Wuebbles, 2013. An asynchronous regional regression model for statistical downscaling of daily climate variables. *International Journal of Climatology*, DOI: 10.1002/joc.3603.

USGCRP, 2017. Fourth National Climate Assessment, Volume I: Climate Science Special Report, Wuebbles, D.J., D.W. Fahey, K.A. Hibbard, D.J. Dokken, B.C. Stewart, and T.K. Maycock (eds.). U.S. Global Change Research Program, Washington, D.C., USA, 470 pp, doi: 10.7930/J0J964J6.